ORNL/TM-2015/539

Oak Ridge National Laboratory Development of ODS FeCrAl Alloys For Accident-Tolerant Fuel Cladding

Sebastien Dryepondt
Kinga A. Unocic
David T. Hoelzer
Bruce A. Pint

September 18, 2015

OAK RIDGE NATIONAL LABORATORY
MANAGED BY UT-BATTELLE FOR THE US DEPARTMENT OF ENERGY

ORNL/TM-2015/539

FCRD Advanced Fuels Campaign

Development of ODS FeCrAl alloys for accident-tolerant fuel cladding

Sebastien Dryepondt
Kinga A. Unocic
David T. Hoelzer
Bruce A. Pint

Date Published:

September 2015

Prepared by
OAK RIDGE NATIONAL LABORATORY
Oak Ridge, Tennessee 37831-6283

managed by
UT-BATTELLE, LLC
for the
US DEPARTMENT OF ENERGY
under contract DE-AC05-00OR22725

CONTENTS

Page

LIST OF FIGURES

Figure **Page**

LIST OF TABLES

Table **Page**

EXECUTIVE SUMMARY

FeCrAl alloys are prime candidates for accident-tolerant fuel cladding due to their excellent oxidation resistance up to 1400ºC and good mechanical properties at intermediate temperature. Former commercial oxide dispersion strengthened (ODS) FeCrAl alloys such as PM2000 exhibit significantly better tensile strength than wrought FeCrAl alloys, which would allow the fabrication of a very thin (~250μm) ODS FeCrAl cladding with sufficient mechanical performance and also a reduction of the potential neutronic penalty due to the replacement of Zr-based alloys by Fe-based alloys. Several Fe-12-Cr-5Al ODS alloys were fabricated by ball milling FeCrAl powders with Y_2O_3 and additional oxides such as TiO_2 or ZrO_2. The new Fe-12Cr-5Al ODS alloys showed excellent tensile strength up to 800ºC but limited ductility. Good oxidation resistance in steam at 1200 and 1400ºC was observed except for one ODS FeCrAl alloy containing Ti. Rolling trials were conducted at 300, 600 and 800ºC to simulate the fabrication of thin tube cladding and plate thickness of ~0.6mm was reached before the formation of multiple edge cracks. Hardness measurements at different stages of the rolling process, before and after annealing for 1h at 1000ºC, showed that a thinner plate thickness could likely be achieved by using a multi-step approach combining warm rolling and high temperature annealing. Finally, new Fe-10-12Cr-5.5-6Al-Z gas atomized powders have been purchased to fabricate the second generation of low-Cr ODS FeCrAl alloys. The main goals are to assess the effect of O, C, N and Zr contents on the ODS FeCrAl microstructure and mechanical properties, and to optimize the fabrication process to improve the ductility of the 2nd gen ODS FeCrAl while maintaining good mechanical strength and oxidation resistance.
This report has been submitted as fulfillment of milestone M2FT-15OR0202281 titled, “Report on progress and properties of first generation ODS FeCrAl alloys for ATF cladding” for the Department of Energy Office of Nuclear Energy, Advanced Fuel Campaign of the Fuel Cycle R&D program.

1. INTRODUCTION

After the Fukushima Daiichi accident, research programs were initiated to develop new accident-tolerant fuel cladding materials.[1,2] Advanced FeCrAl alloys are among the leading candidates due to their excellent oxidation resistance at temperature up to 1450ºC in steam,[3-5] and recent work has shown their mechanical properties at T<900ºC can be improved by grain size control and second phase strengthening.[6] Oxide dispersion strengthened (ODS) FeCrAl alloys are also of great interest due to a similar high temperature steam resistance as wrought FeCrAl alloys but superior mechanical strength. Good mechanical properties would allow for thinner fuel cladding, down to ~300μm for wrought FeCrAl alloys and ~250μm for ODS FeCrAl alloys, and would therefore decrease the neutronic penalty from the replacement of Zr-based alloys by Fe-based alloys.[7]

Several ODS alloys based on Fe-(12-15)Cr-(4-5)Al, in weight percent, containing minor additions such Zr, Ti or Mo were developed at ORNL for both accident tolerant fuel cladding and fusion applications. [5, 8-9]. The Cr content in these ODS alloys was decreased from ~20wt% in former commercial ODS FeCrAl alloys such as MA956 and PM2000 to less than 15wt% in order to limit the formation of brittle α'-Cr-rich phase upon irradiation at low temperature. These alloys showed good oxidation resistance in steam up to 1300-1450ºC, very high yield strength and ultimate tensile strength (UTS) up to 800ºC, but limited ductility at all temperatures. In addition, a recent irradiation study on wrought Fe-(12-17.5)Cr-(3-5)Al revealed that the alloy Cr content needs to be kept below ~12wt% to avoid the formation of the brittle α'-Cr-rich phase.[10] Fe-12Cr-5Al-Y-O (+Zr or Ti) ODS alloys have therefore been the focus of this project for the past year.

The microstructure and tensile properties of the 4 ODS Fe-12Cr-5Al alloys is first compared with the microstructure and mechanical properties of commercial ODS PM2000 alloy (Fe-20Cr-5Al) or recently developed ODS SOC-9 and SOC-14 Japanese alloys (Fe-15Cr-4Al).[11-13] Oxide scales grown in steam at 1200 and 1400ºC at the surface of these ODS Fe-12Cr-5Al alloys were also characterized and compared with scales formed on PM2000 alloys and wrought Fe-(12-20)Cr-5Al alloys tested under similar conditions. To assess tube fabrication feasibility, rolling trials were conducted on a Fe-12Cr-5Al-Zr alloy at 300, 600 and 800ºC. Finally, new gas atomized powders were procured and ball milled to fabricate a second generation of Fe-(10-12)Cr-(5.5-6)Al ODS FeCrAl alloys.

2. EXPERIMENTAL PROCEDURE

2.1 Materials

Fe-12Cr-5Al gas atomized powder was purchased from ATI Metal Powders with a powder size ranging from 45 to 150μm. A Zoz CM08 Simoloyer was used to ball mill for 40h in Ar atmosphere 1 kg batches of Fe-12Cr-5Al with Y_2O_3 powder (125Y alloy), Y_2O_3 + TiO_2 powder (125YT alloy), Y_2O_3 + ZrO_2 powder (125YZ alloy) and Y_2O_3 + FeO powder (125YF alloy). The ball milled powder was then degassed at 300ºC for 24h in an extrusion can, sealed, heated for 1h at 950ºC, and finally extruded at the same temperature. The compositions of the resulting alloys, and the original gas atomized powder are given in Table 1. Alloy 125Y was the first alloy produced and it contains higher level of C and N. This alloy also showed in many cases poor oxidation resistance at temperature as low as 1200ºC, which raised concern of contamination with FeCr powder present in the chamber before ball milling.

A PM2000 rod 30mm in diameter (PM2000 Plansee) and 20kg of PM2000 powder were purchased from Plansee. Approximately 1kg of the powder was extruded at 950ºC following the same procedure as for the Fe-12Cr-5.5Al alloys, and the resulting alloy was named PM2000 ORNL. As can be seen in Table 1, the composition of the two PM2000 alloys is very similar to each other.

For the second generation of ODS FeCrAl alloys, four new batches of powder were purchased and the chemical compositions provided by ATI Metal Powder are given in Table 2. The Al content was increased to ~5.5-6wt% and ~6.5wt%, for the powders containing 12 and 10wt% Cr, respectively. Zirconium at 0.15 to 0.5wt% was added in the gas atomized powder, with one powder containing also 0.15wt% Ti. The 12Cr-5.5Al-0.5Zr powder was ball milled with 0.3wt% Y_2O_3 powder for 40h using the CM08 and the same procedure as that for the first generation gas atomized powder. Approximately 200g of 10Cr-6Al-0.3Zr powder was ball milled for either 10h or 40h with 0.3wt% Y_2O_3 powder using a smaller Zoz CM01 Simoloyer. The chemical composition of the ODS powders after ball milling are included in Table 2.

Table 1: Alloys composition measured by ICP spectroscopy, combustion and IGF analysis for the first generation of ODS FeCrAl alloys and former commercial PM2000 alloys

Wt %	Fe	Cr	Al	Ti	Y	C (ppm)	N (ppm)	O (ppm)	S (ppm)	Other
125 Powder	82.8	12.1	5			31	10	64	<3	0.004Si
125Y	83.3	11.4	4.8	0.01	0.19	380	455	842	20	
125YZ	82.8	11.51	4.86	<0.01	0.18	250	161	1920	10	0.3Zr, 0.01Hf
125YT	82.4	12	4.9	0.2	0.16	350	140	2220	30	
125YF	83	11.67	4.73	0.01	0.19	200	202	1920	30	
PM2000 ORNL	74.66	18.77	5.34	0.45	0.39	20	67	2440	7	0.02Si
PM2000 Plansee	74.12	19.13	5.46	0.48	0.39	14	86	2480	8	0.02Si

Table 2: Composition of the 2nd generation gas atomized powders measured by ATI Metal Powder and composition of the same powders after ball milling measured by ICP spectroscopy, combustion and IGF analysis.

		Fe	Cr	Al	Zr	Y	C (ppm)	N (ppm)	O (ppm)	S (ppm)	Other
Gas Atomized	12Cr-5.5Al-0.5Zr Powder	81.8	11.9	5.6	0.54		20	20	140	20	0.01Si
	12Cr-5.5Al-Zr-Ti Powder	81.3	12.2	5.9	0.24		40	20	130	30	0.14Ti-0.01Si
	10Cr-6Al-0.3Zr Powder	83.1	10	6.4	0.29		40	20	190	30	
	10Cr-6Al-0.15Zr Powder	83.1	10.2	6.3	0.15		40	20	190	20	0.01Si
Ball Milled	125.5ZY 40h	81.06	11.97	5.52	0.49	0.19	190	133	1360	50	0.22Ni-0.14Mn
	106ZY 40h	81.08	9.95	5.98	0.3	0.2	250	610	1490	40	0.04Co-0.03Si
	106ZY 10h	83.07	10.05	6.13	0.3	0.2	70	127	132	20	0.03Co

2.2 Tensile testing

Sub-sized tensile specimens (SS-3) with a 7.62 mm long and 0.762 or 1mm thick gage section were machined along the extrusion direction. Tensile testing was conducting from room temperature to 740ºC or 800ºC at a deformation rate of $10^{-3}s^{-1}$ with an MTS hydraulic or an Instron electro-mechanical machine.

2.3 Oxidation testing

Rectangular ~20x10x1-1.5mm coupons were polished to a 600 grit surface finish and then cleaned in acetone and methanol. Isothermal oxidation experiments were conducted at 1200ºC in 100% steam using a magnetic suspension Rubotherm DynTHERM thermogravimetric analyzer (TGA). A high temperature steam furnace was used to conduct oxidation testing at 1400ºC in steam. The specimens were heated up with a constant heating rate in 3h to 1400ºC in an Ar environment and then exposed to steam flowing at a rate of 200ml/h for 4h.

2.4 Heat treatment, hardness measurement and warm rolling

Vickers hardness was measured using a 200 or 500g load for all specimens before and after annealing for 1h at 1000 or 1200ºC. The 125YZ plates with a size of 20x16x3mm were annealed for 1h at 1000ºC and then rolled to a 50% thickness reduction at 300 or 600ºC. Warm rolling at 300 and 600ºC was then continued until the appearance of edge cracks, which occurred after a total thickness reduction of ~80% and final sheet thicknesses of 500 to 600μm. Similar hot rolling was carried out at 800ºC with a 125YZ plate with 5mm thickness and the final thickness before cracking was again ~600 μm, for a total thickness reduction close to 90%.

2.5 Microstructure characterization

As extruded, annealed and oxidized coupons were mounted in an epoxy resin and then polished using standard metallography techniques. The microstructure of the alloy and/or the oxide scale was then characterized using a JEOL model 6500 Field Emission Gun Scanning Electron Microscope (FEG-SEM). The transmission electron microscopy (TEM) specimens were extracted by Focused Ion Beam (FIB, Hitachi model NB500) using the in-situ lift-out method. TEM microstructure analysis was conducted using either a Philips model CM200 FEGTEM/STEM (Scanning TEM) or a FEI Talos F200X (S/TEM).

3. RESULTS

3.1 Microstructure characterization

As can be seen in Figure 1a-1b, a very fine grain structure was observed for all the Fe-12Cr-5Al alloys with the presence of larger grains and a network of Al_2O_3 stringers. A similar microstructure was previously reported for Fe-15Cr-5Al ODS FeCrAl alloys.[8] SEM and/or TEM images were used to estimate the grain size for the Fe-12Cr-5Al and PM2000 alloys, both along and perpendicular to the extrusion direction, and the results are summarized in Table 3. Alloys 125YT and 125YZ exhibited very small grain sizes, ~130nm and ~220nm, respectively. The grain size for alloy 125YF was slightly higher, ~450nm, and alloy 125Y showed a grain size approaching the grain size of the PM2000 alloys, ~650nm. For all these alloys, the grain aspect ratio (GAR) was quite small, i.e. less than 1.6.

Very small nano precipitates in the grain and at the grain boundary (Figure 2) were revealed by TEM, and the average precipitate size and precipitate number density were added in Table 3 for alloy 125Y, 125YT and 125YZ. For the three alloys, the precipitate size was only 2 to 3nm and the precipitate number density quite high, especially for alloy 125YT. A more detailed description of the microstructure of alloy 125YZ is reported in reference [14].

Figure 3a compares the average grain size for alloy 125Y, 125YZ and 125YT with the grain size of two ODS FeCrAl alloys developed in Japan, SOC-9 (Fe–15.5Cr–2W–0.1Ti–4Al–0.35Y_2O_3) extruded at 1050ºC or 1150ºC and SOC-14 (Fe–15Cr–2W–0.1Ti–4Al–0.63Zr–0.35Y_2O_3) extruded at 1150ºC. [11-13]. Consistent with the findings of Dou et al.,[12] the grain size along the extrusion direction decreased from ~3μm at 1050ºC to less than 1 μm at 950ºC. However, decreasing the extrusion temperature from 1050ºC to 950ºC had a limited impact on the grain size perpendicular to the extrusion direction, which explains the low grain aspect ratio for the Fe-12Cr-5Al alloys. Figure 3b shows that decreasing the extrusion temperature to 950ºC also increased the precipitate number density, but the precipitate mean diameter reached a limit of ~2 to 3nm.

TEM characterization indicated that the nano precipitates in the 125Y and 125YT alloys are likely YAG ($Y_3Al_5O_{12}$) and Al_2TiO_5, respectively. Contrary to what was observed by Dou et al. with the SOC-14 alloy,[13] precipitates in the 125YZ alloy could not be clearly identified as $Y_4Zr_3O_{12}$.[14] The chemical maps generated using the new FEI Talos F200X (Figure 4) revealed that the nano precipitates are likely complex Al-Y-Zr-O oxides.

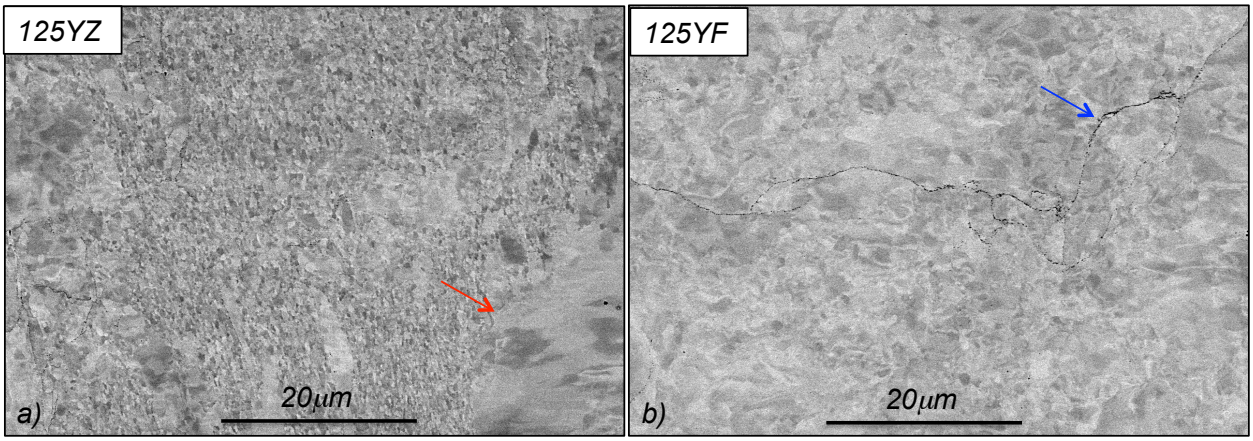

Fig. 1: Backscattered SEM micrographs after extrusion showing a very small grain size for a) alloy 125YZ and b) alloy 125YF. The red arrow indicates an area with larger grains and the blue arrow highlights the presence of alumina stringers.

Table 3: Grain size, grain aspect ratio (GAR), precipitate size and precipitate number density for the Fe-12Cr-5Al alloys and PM2000 alloys.

	Average Grain Size (μm)		GAR	Ave. Precipitate Size (nm)	Precipitate Number Density (m^{-3})
Alloy	Parallel to ED	Normal to ED			
125Y	0.83	0.56	1.48	2.4	1.41×10^{23}
125YT	0.14	0.12	1.17	2.2	6.78×10^{23}
125YZ	0.27	0.17	1.59	2.9	2.51×10^{23}
125YF	0.46	0.42	1.08		
PM2000 Plansee	1	0.7	1.43		
PM2000 ORNL	0.7				

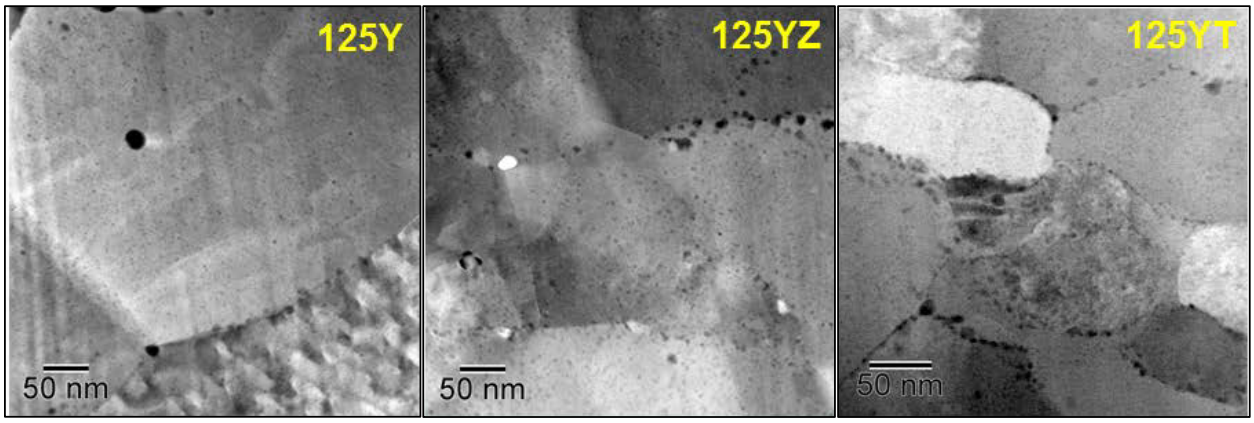

Fig. 2: TEM micrographs after extrusion, a) alloy 125Y, b) alloy 125YZ, c) alloy 125YT, showing a large number of small precipitates in the grain and at grain boundary.

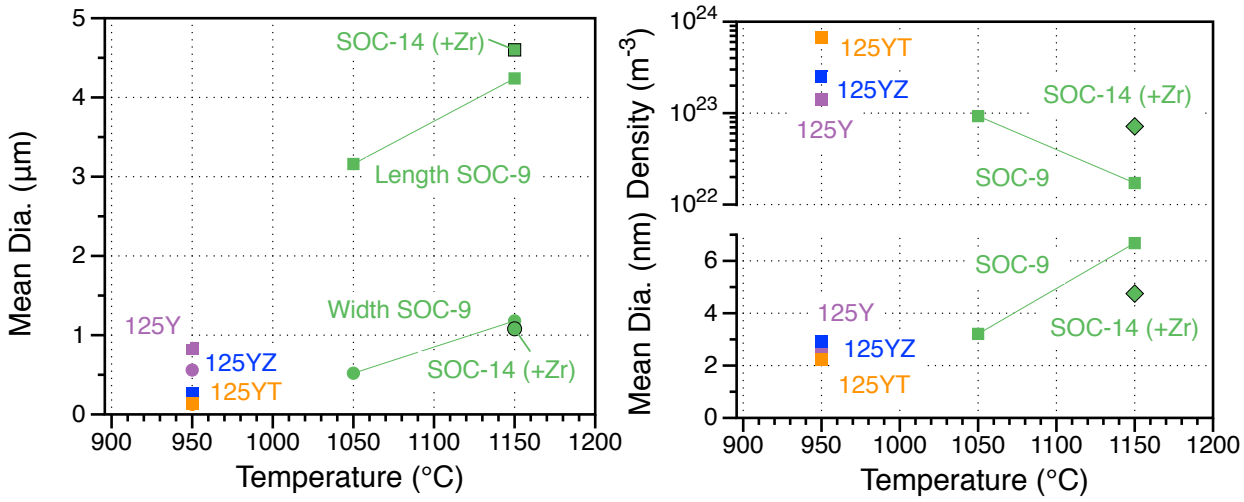

Fig. 3: Microstructure comparison based on extrusion temperature between the Fe-12Cr-5Al alloys developed at ORNL and the SOC (15Cr-5Al-2W) Japanese alloys, a) Average grain size, b) Precipitate number density and average size.

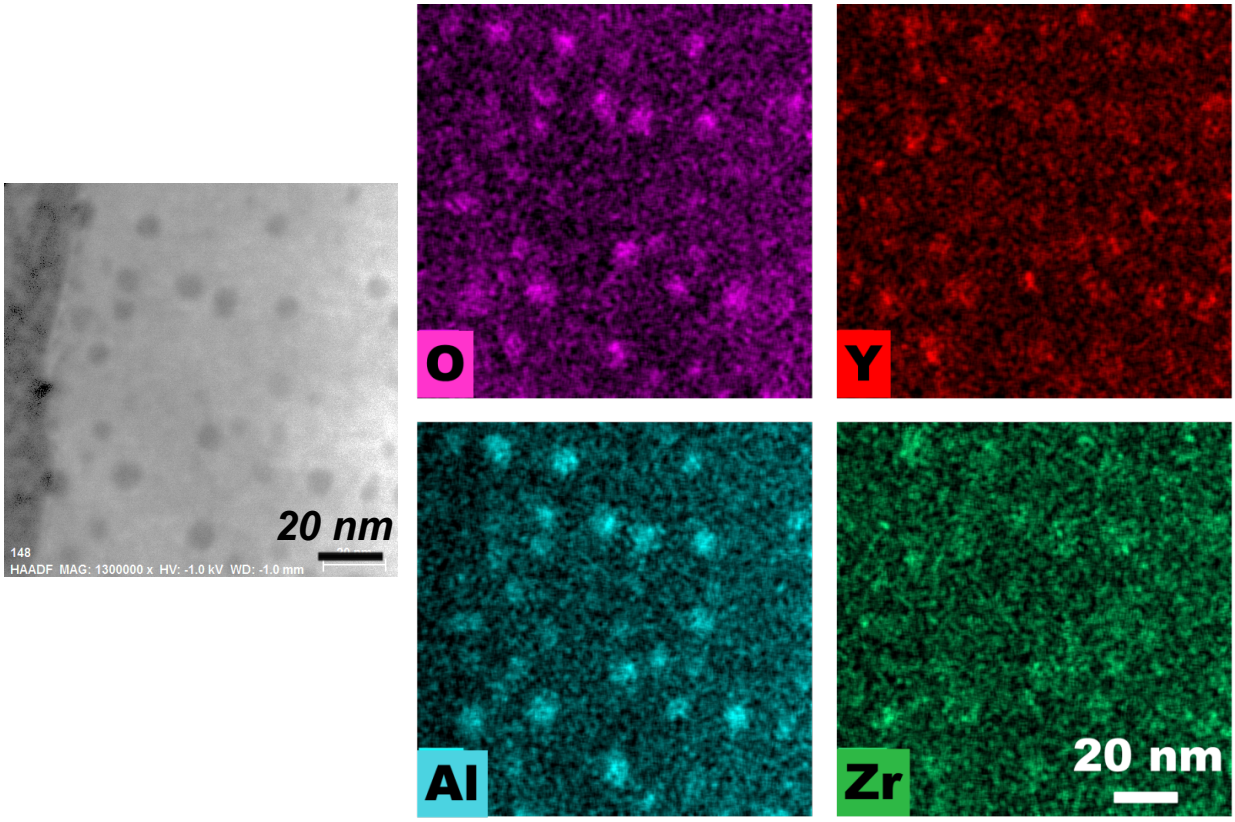

Fig. 4: Chemical mapping of the complex Al-Y-Zr-O nano oxides formed after extrusion in alloy 125YZ.

3.2 Tensile Properties

The ultimate tensile strength (UTS) and total plastic deformation for the Fe-12Cr-5Al alloys and PM2000 ORNL alloys from room temperature to 740 or 800ºC are presented in Figure 5. The 125YF and 125YZ alloys exhibited tensile properties similar to the tensile properties for the Fe-15Cr-5Al ODS alloys developed and characterized previously [8]. The UTS for the PM2000 ORNL alloy is similar to the UTS of alloy 125YZ up to ~600ºC, but is significantly lower at 800ºC. This alloy, however, showed a better ductility at all temperatures. The tensile properties of alloy 125Y were lower at all temperatures compared with those for alloy 125YZ and 125YF and there was a slight ductility improvement. On the contrary, very high tensile properties were measured for alloy 125YT at temperatures below 400ºC but the alloy was very brittle at low temperature. Overall, the tensile strength of the Fe-12Cr-5Al alloys at temperatures below ~500ºC seems to increase with decreasing grain size.

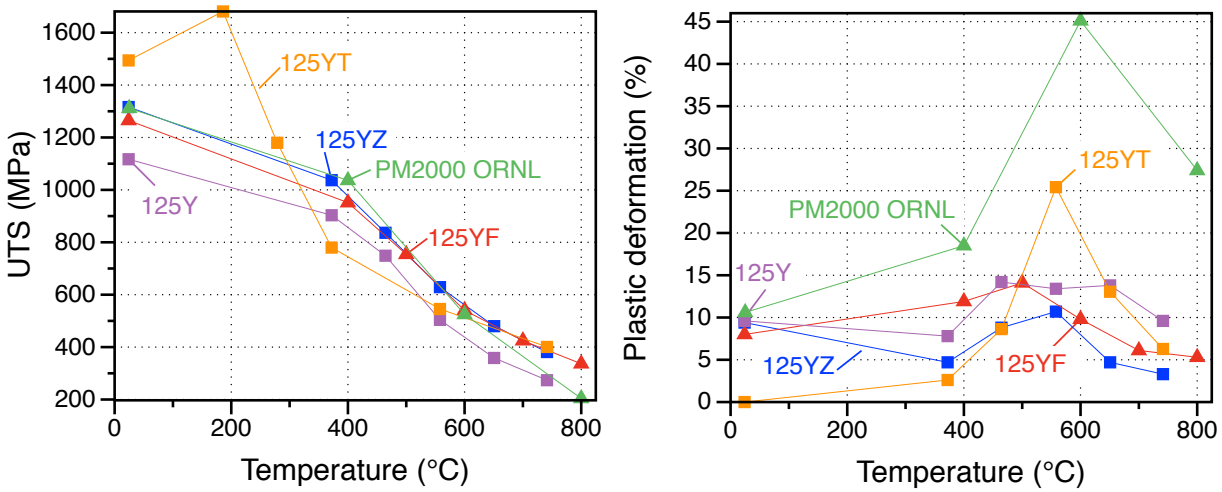

Fig. 5: Tensile properties for the Fe-12Cr-5Al alloys and PM2000 ORNL from room to 740 or 800ºC, a) Ultimate tensile strength, b) Plastic deformation at rupture.

3.3 High Temperature oxidation

High temperature mass gains at 1200ºC in air and steam have been reported previously for Fe-15Cr-5Al alloys and alloy 125YZ, [8] and the measured rate constants k_p were slightly higher in steam. The 125Y alloy showed higher mass gains at high temperature compared with the other Fe-12Cr5-5Al alloys most likely because of contamination with FeCr powder during ball milling. Cross-section micrographs of the oxide scale formed in steam after 4h at 1200ºC for alloy 125YZ, 125YT and a wrought Fe-12Cr-5Al alloy are shown in Figure 6.

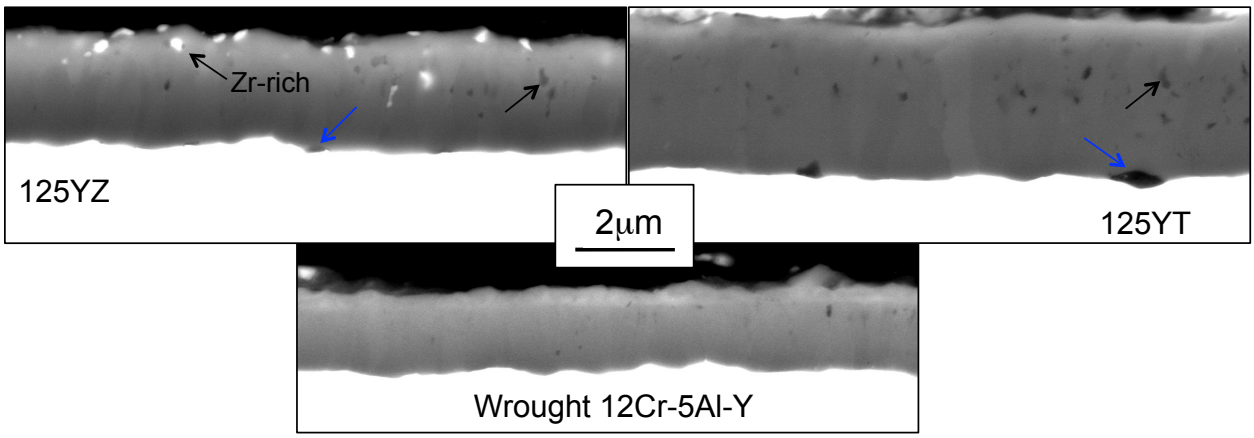

Fig. 6: Backscattered SEM micrographs of the oxide scale formed after 4h at 1200ºC in steam, a) alloy 125YZ, b) alloy 125YT and c) wrought Fe-12Cr-5Al alloy. Black arrows show Zr-rich precipitates or small voids in the scale. Blue arrows highlight interfacial voids.

The oxide scale thickness was ~ 1.75μm for the wrought FeCrAl alloy, ~2.5 μm for 125YZ alloy [15] and 3 to 3.5 μm for 125YT alloy. Zirconium-rich oxide precipitates were observed in the 125YZ alloy and many small voids (blacks arrows in Figure 6a and 6b) in the scale grown on alloys 125YZ and 125YT. These defects in the scale are most likely the reason for the faster alumina growth rate for these two alloys. In addition, voids were observed at the scale/metal interface for the two ODS alloys.[15]

The Fe-12Cr-5Al alloys and PM2000 alloys were also tested at 1400ºC in steam for 4h. At this temperature, seven out of eight wrought Fe-(10-20)Cr-(5-8)Al coupons went into breakaway oxidation and were completely oxidized after 4h. The 125YZ, 125YF and PM2000 ORNL alloys showed low mass gains after 4h at 1400ºC in steam, but the 125YT coupon failed the test. The PM2000 Plansee alloy was tested in the as-received small grain and recrystallized very large grain states. Annealing alloy PM2000 Plansee for 1h at 1380ºC led to alloy recrystallization and the formation of grain several millimeters in size. In the small grain state, one PM2000 coupon passed and another failed the 1400ºC 4h test. However in the recrystallized state, alloy PM2000 Plansee exhibited only low mass gain after 4h at 1400ºC and 4h at 1450ºC. All the other ODS alloys went into breakaway oxidation when exposed to steam at 1450ºC for more than 1h.

The microstructure of alloy 125YZ in the bulk and at the specimen surface after 4h at 1400ºC in steam are shown in Figure 7a and 7b, respectively. Significant grain growth occurred during the test and large voids formed in the alloy most likely because of the gas entrapped during the ball milling process. Similar to what was observed at 1200ºC, Zr-rich particles and small voids were present in the alumina scale, as well as voids at the scale/alloy interface. In addition, the scale/alloy interface appeared very convoluted because of the growth stress in the alumina scale and the resulting deformation of the weak substrate at 1400ºC. The oxide scale grown on alloy 125YF was also very convoluted and more fragmented compared with that on 125YZ (Figure 8a). As can be seen in Figure 8b, the scale was locally thicker and very porous, with numerous small particles at the void edges. Some metal was also entrapped in the alumina scale.

The oxide scale features for the scales formed on the PM2000 alloys after 4h at 1400ºC are summarized in Figure 9. A convoluted oxide scale with very few voids or Y-rich precipitates was observed on the PM2000 Plansee large grain material (Figure 9a). The scale formed on the PM2000 ORNL alloy was also convoluted and there were large voids which led to scale cracking, mostly along grain boundaries, and local separation of the oxide top layer (Figure 9b). Figure 9c and 9d shows that the oxide scale formed on the small grain PM2000 Plansee was often very similar to the scale grown on the large grain PM2000 alloy, but regions with large voids and scale separation were also noticed.

In conclusion two degradation mechanisms of the alumina scale at 1400ºC in steam were observed: the mechanical deformation of the scale/alloy interface in conjunction with interface void formation that could lead to scale spalling at temperature (even before cooling), and the microstructure degradation of the alumina scale associated with the formation of large voids and partial separation of the scale.

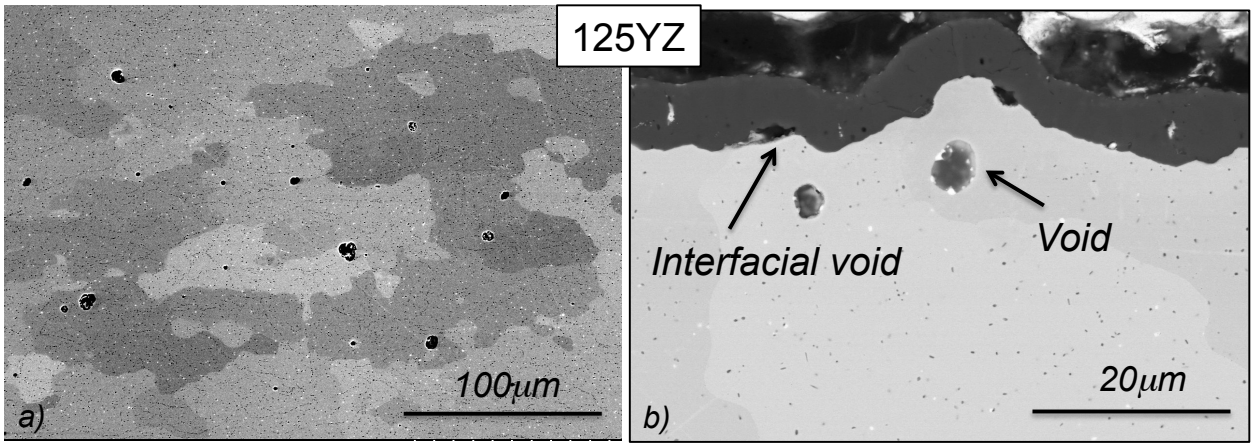

Fig. 7: Backscattered SEM micrographs of alloy 125YZ after exposure for 4h in steam at 1400ºC, a) bulk of the alloy, b) oxide scale.

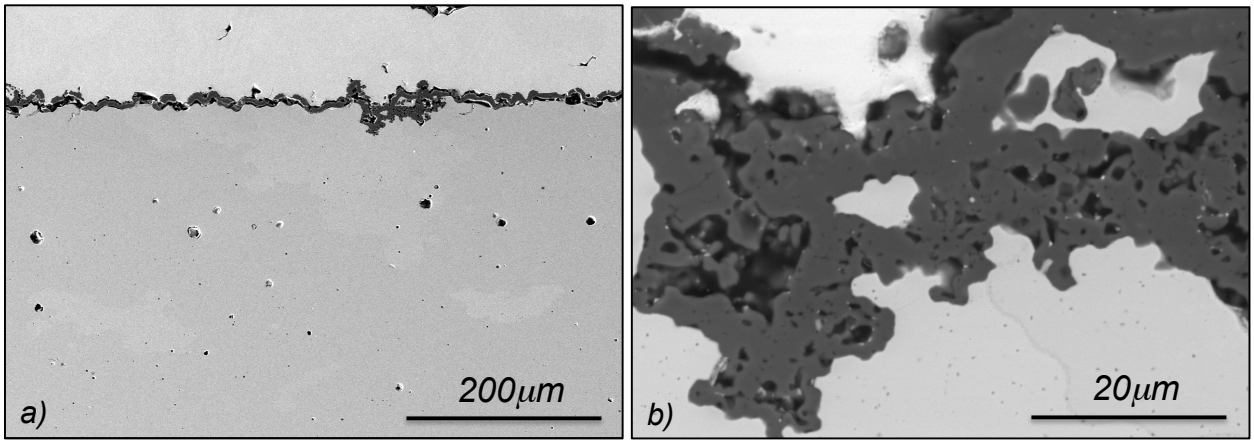

Fig. 8: Backscattered SEM micrographs of alloy 125YF after exposure for 4h in steam at 1400ºC, a) scale overview, b) degraded alumina scale.

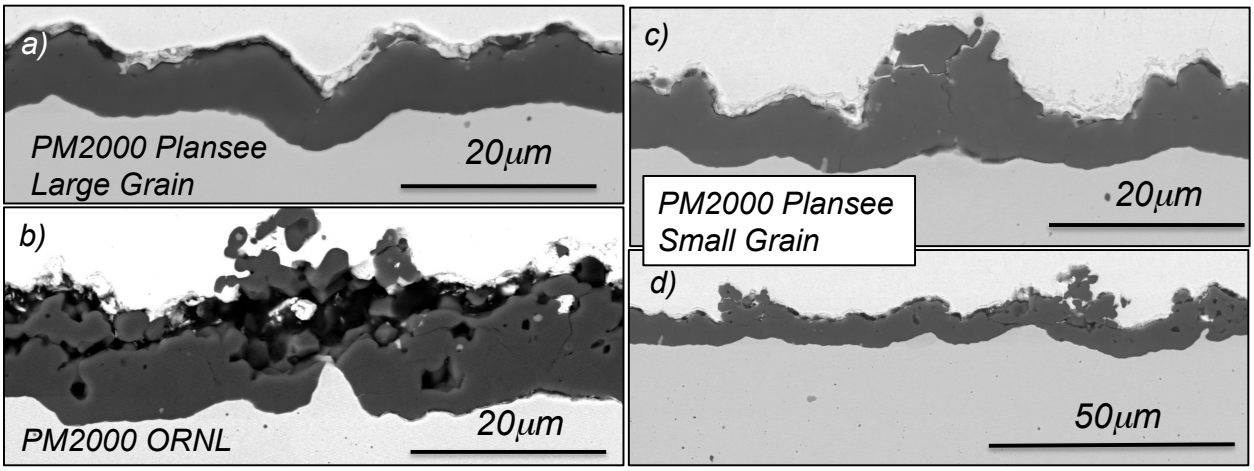

Fig. 9: Backscattered SEM micrographs of PM2000 alloys after exposure for 4h in steam at 1400ºC, a) Large grain recrystallized PM2000 Plansee, b) PM2000 ORNL, c) and d) Small grain PM2000 Plansee.

3.4 Hardness measurement and warm/hot rolling of alloy 125YZ

Rolling trials on alloy 125YZ were selected as a first step to assess the fabrication feasibility of thin ODS FeCrAl tubes. As expected from the very high tensile strength measured for the Fe-12Cr-5Al alloys, the hardness of these alloys was very high except for alloy 125Y (Figure 10). Also, work on wrought FeCrAl alloys has shown that hardness values above ~350Hv degraded significantly wrought FeCrAl fabricability. Therefore, the Fe-12Cr-5Al alloys were heat treated at 1000 or 1200ºC and the resulting hardness values are shown in Figure 10. The hardness values of the 125YZ, 125YT and 125YF alloys were slightly lower than 400Hv after 1h at 1000ºC, but decreased to ~300Hv or less after annealing for 1h at 1200ºC. Significant precipitate coarsening was observed after the 1h at 1200ºC heat treatment. One hour at 1000ºC was therefore selected as a softening heat treatment, and small 125YZ sheets were rolled at 300, 600 and 800ºC first to a total thickness reduction of 50%, and then until edge cracks appeared. The final thickness was between 500 and 650 μm for all the rolled sheets, which corresponded to a reduction of ~80% (~90% at 800ºC).

Figure 11 shows that the hardness value increased after 50% rolling at 300ºC but decreased after 80% rolling at 300ºC. Opposite results were observed at 600 and 800ºC, with a significant decrease of hardness after 50% rolling and then a slight hardness increase after 80% rolling. It is worth noting that at all rolling temperatures and after both 50 and 80% total thickness reduction, annealing the sheet for 1h at 1000ºC led to a decrease of the hardness value down to ~315Hv. Further research is needed to understand the impact of the 1h at 1000ºC anneals on the microstructure and tensile properties of the rolled 125YZ sheets, but adding annealing steps at temperature ~1000ºC during the rolling process as was proposed by Ukai et al. could allow for thinner sheet thickness without edge cracking. [16]

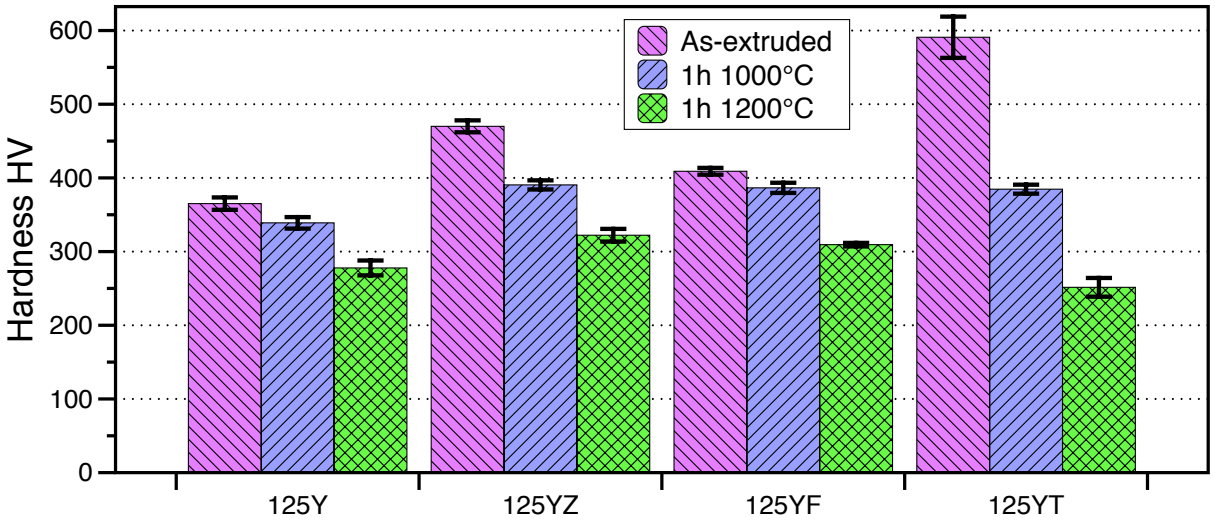

Fig. 10: Vickers hardness measurement for the Fe-12Cr-5Al alloys after extrusion and exposure for 1h at 1000ºC or 1200ºC.

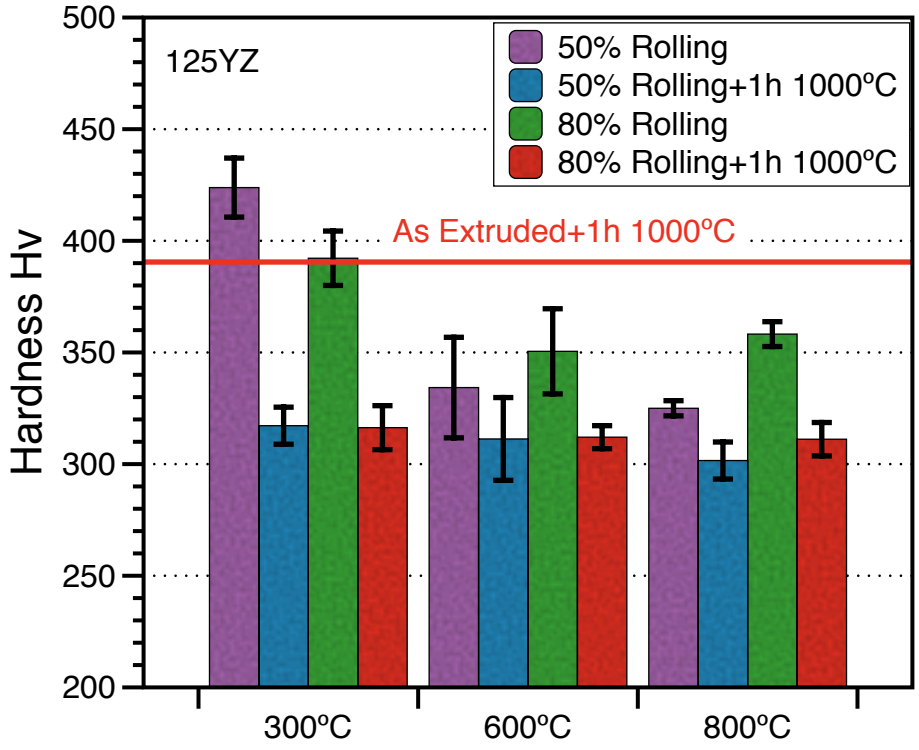

Fig. 11: Vickers hardness measurement before and after annealing at 1000ºC for 125YZ sheets rolled at 300, 600 and 800ºC for a total thickness reduction of 50% and ~80% (~90% at 800ºC).

4. 2nd GENERATION OF ODS FeCrAl ALLOYS AND FUTURE WORK

Based on the results from the first generation of ODS Fe-12Cr-15Cr alloys and research on wrought FeCrAl alloys, 4 new batches of FeCrAlZr powders were purchased. The first main change is the addition in the gas atomized powders of Zr. Ball milling the Fe-12Cr-5Al powder with Y_2O_3 and ZrO_2 led to a high oxygen concentration in the alloy and the oxygen content was found to be a critical parameter to obtain a high number density of nano-oxide precipitates in a 14YWT ODS alloy.[17] Comparison between Table 1 and Table 2 shows that the oxygen concentrations in the FeCrAlZr powders ball milled with Y_2O_3 powder were indeed lower than in alloy 125YZ. In future ball milling runs, the oxygen concentration could always be increased, if deemed appropriate, by adding small amount of FeO powder.

The Zr concentration is also likely to play a significant role in the nano precipitates size and number density, and the Zr content was varied in the new powders from 0.15wt% to 0.5wt%. However, high temperature oxidation testing will be required to verify that 0.5%wt Zr does not lead to the detrimental formation of ZrO_2 precipitates in the oxide scale and the degradation of the alloy oxidation performance. Recent irradiation work has demonstrated that FeCrAl embrittlement is directly related to the Cr content.[10] In the 2nd gen ODS FeCAl alloys, the Cr concentration was limited to 12 or 10%wt, and the Al concentration was increased to 5.5wt% for the 12Cr alloy and 6wt% for the 10Cr alloy to enhance the alloy oxidation performance.

Figure 12 compares the tensile properties of alloy 125YZ, the PM2000 alloys, and two wrought FeCrAl alloys. The UTS of alloy 125YZ is considerably superior at all temperatures to the UTS of the standard FeCrAl alloy or even the second generation wrought FeCrAl alloy developed at ORNL. The main issue that needs to be solved with the 2nd generation ODS FeCrAl alloys is the lack of ductility.
Alloy PM2000 ORNL is much more ductile than alloy 125YZ at >~200ºC, and showed similar tensile strength at <600ºC. Alloy PM2000 Plansee was even more ductile, but the alloy tensile strength was lower than the tensile strength of alloy 125YZ or PM2000 ORNL. The fabrication process of alloy PM2000 Plansee is unknown, but comparison between the two PM2000 alloys indicates that two ODS alloys of very similar chemistry can have quite different mechanical properties depending on the fabrication process. The impact of extrusion temperature and post thermo-mechanical treatment on the 2nd gen of ODS alloys will be optimized to improve the alloy ductility. Finally, it is worth noting that the extremely low N and C concentrations in the two ODS alloys compared with those in the Fe-12Cr-5Al alloys could play a role in the alloys good ductility. As can be seen in Table 2, decreasing the ball milling time led to a decrease of C and N ingress during ball milling. The effect of ball milling time on the alloy mechanical properties will therefore also be evaluated.

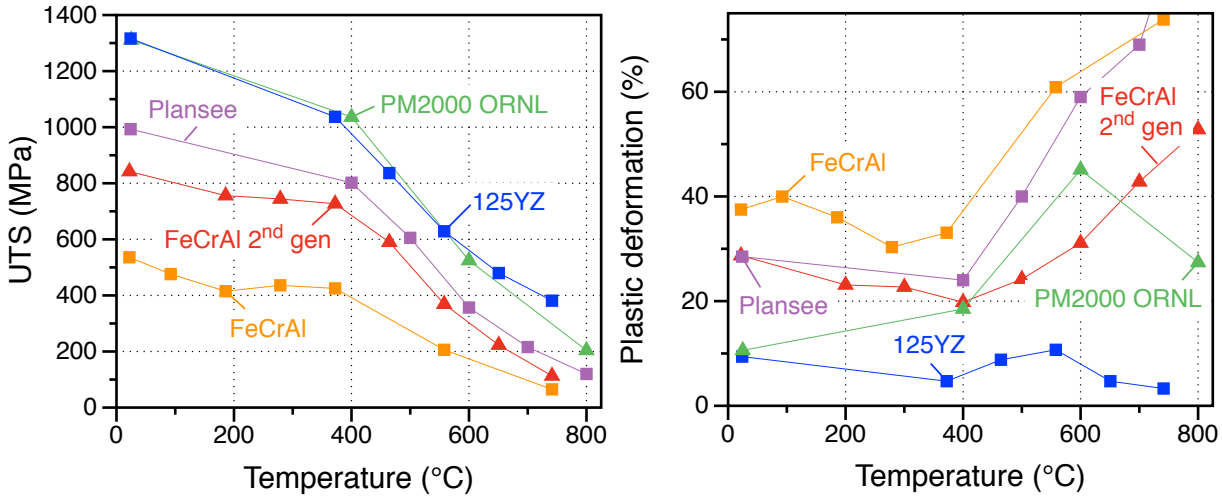

Fig. 12: Tensile properties of alloy 125YZ, two PM2000 Plansee alloys and two wrought FeCrAl alloys, a) Ultimate tensile strength, b) Plastic deformation at rupture.

5. CONCLUSION

Several ODS Fe-12Cr-5Al alloys fabricated at ORNL by ball milling exhibited excellent tensile strength but limited ductility up to 800ºC, and very good oxidation resistance in steam up to 1400ºC. Rolling trials were conducted on alloy 125YZ at 300, 600 and 800ºC and sheets ~500-650µm thick were fabricated before edge cracking started to appear. A second generation of ODS FeCrAlZr alloys is currently being developed with a focus on alloy ductility. Special attention will be paid to the new alloys chemistry, in particular the O, C and N concentration. The powder ball milling and consolidation process will also be optimized to improve alloy ductility.

6. ACKNOWLEDGMENTS

The authors would like to thank J. Turan, C. Massey, M. Howell, T Jordan, T Geer, T. Lowe, C. Stevens, M. Stephens, and D. Harper for their help with the experimental work. They want also to acknowledge Y. Yamamoto and D.F. Wilson for reviewing the manuscript. This research was sponsored by the U.S. Department of Energy, FCRD Advanced Fuels Campaign Program.

7. REFERENCES

[1] S.J. Zinkle, K.A. Terrani, J.C. Gehin, L.J. Ott, L.L. Snead, "Accident tolerant fuels for LWRs: A perspective", Journal of Nuclear Materials, 448, 374-379 (2014).
[2] K. A. Terrani, S. J. Zinkle, L. L. Snead, "Advanced oxidation-resistant iron-based alloys for LWR fuel cladding", Journal of Nuclear Materials, 448, 420-435 (2014).
[3] F.H. Stott, G.C. Wood, F.A. Golightly, "The isothermal oxidation behavior of Fe-Cr-Al and Fe-Cr-Al-Y at 1200ºC", Corrosion Science, 19, 869-887 (1979).
[4] T. Cheng, J. R. Keiser, M. P. Brady, K. A. Terrani and B. A. Pint, "Oxidation of fuel

cladding candidate materials in steam environments at high temperature and pressure", Journal of Nuclear Materials, 427, 396-400 (2012).
[5] B. A. Pint, K. A. Unocic and K. A. Terrani, "The Effect of Steam on the High Temperature Oxidation Behavior of Alumina-Forming Alloys", Materials at High Temperatures, 32, 28-35 (2015).
[6] Y. Yamamoto, B.A. Pint, K.A. Terrani, K.G. Field, L.L. Snead, "Letter report documenting identifying billets and alloys fabricated for distribution to program" M3FT-13OR0202291, ORNL/LTR-2013/322, Oak Ridge National Laboratory (2013).
[7] N.M. George, K.A. Terrani, J.J. Powers, "Neutronic analysis of candidate accident-tolerant iron alloy cladding concepts", ORNL report TM-2013/121 (2013).
[8] S. Dryepondt, K. A. Unocic, D. T. Hoelzer, B. A. Pint, "Advanced ODS FeCrAl Alloys For Accident-Tolerant Fuel Cladding", ORNL report, ORNL/TM-2014/380 (2014).
[9] B. A. Pint, S. Dryepondt, K. A. Unocic and D. T. Hoelzer, "Development of ODS FeCrAl for Compatibility in Fusion and Fission Energy Applications", JOM 66 (2014) 2458.
[10] K. G. Field, X. Hu, K. C. Littrell, Y. Yamamoto, L. L. Snead, "Radiation tolerance of neutron-irradiated model FeCrAl alloys", Journal of Nuclear Materials, 465, 746-755 (2015).
[11] P. Dou, A. Kimura, T. Okuda, M. Inoue, S. Ukai, S. Ohnuki, T. Fujisawa and F. Abe, "Effects of extrusion temperature on the nano-mesoscopic structure andmechanical properties of an Al-alloyed high-Cr ODS ferritic steel", Journal of Nuclear Materials, 417, 166-170 (2011).
[12] A. Kimura, R. Kasada, N. Iwata, H. Kishimoto, C.H. Zhang, J. Isselin, P. Dou, J.H. Lee, N. Muthukumar, T. Okuda, M Inoue, S. Ukai, S. Ohnuki, T. Fujisawa and T.F. Abe, "Development of Al added high-Cr ODS steels for fuel cladding of next generation nuclear systems", Journal of nuclear materials, 417, 176-179 (2011).
[13] P. Dou, A. Kimura, R. Kasada, T. Okuda, M. Inoue, S. Ukai, S. Ohnuki, T. Fujisawa, F. Abe, "TEM and HRTEM study of oxide particles in an Al-alloyed high-Cr oxide dispersion strengthened steel with Zr addition", Journal of nuclear materials, 444, 441-453 (2014).
[14] D.T. Hoelzer and K.A. Unocic, "The Effect of Zr and Hf on the Microstructure and Tensile Properties of ODS Fe-12Cr-5Al+Y2O3 Ferritic Alloys", Submitted for publication in the Journal of Materials Science, (2015).
[15] K.A. Unocic, D. T. Hoelzer and B. A. Pint, "The Microstructure and environmental resistance of low Cr ODS FeCrAl," Materials at High Temperatures, 32, 123-132 (2015).
[16] S. Ukai, M. Harada, H. Okada, M. Inoue, S. Nomura, S. Shikakura, T. Nishida, M. Fujiwara and K. Asabe, "Tube manufacturing and mechanical properties of oxide dispersion strengthened ferritic steel", Journal of nuclear materials, 204, 74-80 (1993).
[17] N.J. Cunningham,Y. Wu, A. Etienne, E.M. Haney, G.R. Odette, E. Stergar, D.T. Hoelzer, Y.D. Kim, B.D. Wirth and S.A. Maloy, "Effect of bulk oxygen on 14YWT nanostructured ferritic alloys", Journal of nuclear materials, 444, 35-38 (2014).